Research Article | Vol. 7, No. 9 | 1 Sep 2016 | BIOMEDICAL OPTICS EXPRESS 3461
Biomedical Optics EXPRESS

Continuous cerebral hemodynamic measurement during deep hypothermic circulatory arrest

DAVID R. BUSCH,[1,2,*] CRAIG G. RUSIN,[3] WANDA MILLER-HANCE,[4] KATHY KIBLER,[5] WESLEY B. BAKER,[2,6] JEFFREY S. HEINLE,[7] CHARLES D. FRASER,[7] ARJUN G. YODH,[2] DANIEL J. LICHT,[1] AND KENNETH M. BRADY[8]

[1]*Division of Neurology, Department of Pediatrics, Children's Hospital of Philadelphia, Philadelphia, PA, 19104, USA*
[2]*Department of Physics and Astronomy, University of Pennsylvania, Philadelphia, PA 19104, USA*
[3]*Departments of Pediatrics and Cardiology, Baylor College of Medicine, Houston, TX, 77030 USA*
[4]*Department of Pediatric Cardiovascular Anesthesiology, Baylor College of Medicine, Houston, TX, 77030 USA*
[5]*Department of Pediatrics, Texas Children's Hospital, Houston, TX, 77030, USA*
[6]*Department of Anesthesiology and Critical Care, Hospital of the University of Pennsylvania, Philadelphia, PA 19104, USA*
[7]*Department of Surgery, Texas Children's Hospital, Houston, TX, 77030, USA*
[8]*Department of Anesthesiology, Baylor College of Medicine, Houston, TX, 77030, USA*
[*]*drbusch@sdf.org*

Abstract: While survival of children with complex congenital heart defects has improved in recent years, roughly half suffer neurological deficits suspected to be related to cerebral ischemia. Here we report the first demonstration of optical diffuse correlation spectroscopy (DCS) for continuous and non-invasive monitoring of cerebral microvascular blood flow during complex human neonatal or cardiac surgery. Comparison between DCS and Doppler ultrasound flow measurements during deep hypothermia, circulatory arrest, and rewarming were in good agreement. Looking forward, DCS instrumentation, alone and with NIRS, could provide access to flow and metabolic biomarkers needed by clinicians to adjust neuroprotective therapy during surgery.

OCIS codes: (170.3890) Medical optics instrumentation; (170.6935) Tissue characterization.

References and links

1. J. I. Hoffman and S. Kaplan, "The incidence of congenital heart disease," J. Am. Coll. Cardiol. **39**(12), 1890–1900 (2002).
2. E. M. Graham, S. C. Zyblewski, J. W. Phillips, G. S. Shirali, S. M. Bradley, G. A. Forbus, V. M. Bandisode, and A. M. Atz, "Comparison of Norwood shunt types: do the outcomes differ 6 years later?" Ann. Thorac. Surg. **90**(1), 31–35 (2010).
3. A. J. Shillingford, M. M. Glanzman, R. F. Ittenbach, R. R. Clancy, J. W. Gaynor, and G. Wernovsky, "Inattention, hyperactivity, and school performance in a population of school-age children with complex congenital heart disease," Pediatrics **121**(4), e759–e767 (2008).
4. B. S. Marino, P. H. Lipkin, J. W. Newburger, G. Peacock, M. Gerdes, J. W. Gaynor, K. A. Mussatto, K. Uzark, C. S. Goldberg, W. H. Johnson, Jr., J. Li, S. E. Smith, D. C. Bellinger, and W. T. Mahle, "Neurodevelopmental Outcomes in Children With Congenital Heart Disease: Evaluation and Management: A Scientific Statement From the American Heart Association," Circulation **126**, 1143–1172 (2012).
5. M. Y. Naim, J. W. Gaynor, J. Chen, S. C. Nicolson, S. Fuller, T. L. Spray, D. J. Dlugos, R. R. Clancy, L. V. Costa, D. J. Licht, R. Xiao, H. Meldrum, and N. S. Abend, "Subclinical seizures identified by postoperative electroencephalographic monitoring are common after neonatal cardiac surgery," J. Thorac. Cardiovasc. Surg. **150**(1), 169–180 (2015).
6. E. A. Gottlieb, C. D. Fraser, Jr., D. B. Andropoulos, and L. K. Diaz, "Bilateral monitoring of cerebral oxygen saturation results in recognition of aortic cannula malposition during pediatric congenital heart surgery," Paediatr. Anaesth. **16**(7), 787–789 (2006).
7. F. G. Scholl, D. Webb, K. Christian, and D. C. Drinkwater, "Rapid diagnosis of cannula migration by cerebral oximetry in neonatal arch repair," Ann. Thorac. Surg. **82**(1), 325–327 (2006).
8. S. Hyttel-Sorensen, T. W. Hessel, and G. Greisen, "Cerebral near infrared spectroscopy oximetry in extremely preterm infants: phase II randomised clinical trial," J. Clin. Monit. Comput. **350**, 1–7 (2013).
9. T. Aoyagi, "Pulse oximetry: its invention, theory, and future," J. Anesth. **17**(4), 259–266 (2003).

#266921 http://dx.doi.org/10.1364/BOE.7.003461
Journal © 2016 Received 24 May 2016; revised 5 Aug 2016; accepted 8 Aug 2016; published 15 Aug 2016

Biomedical Optics EXPRESS

10. J. T. Elliott, E. A. Wright, K. M. Tichauer, M. Diop, L. B. Morrison, B. W. Pogue, T. Y. Lee, and K. St Lawrence, "Arterial input function of an optical tracer for dynamic contrast enhanced imaging can be determined from pulse oximetry oxygen saturation measurements," Phys. Med. Biol. **57**(24), 8285–8295 (2012).
11. T. Durduran, R. Choe, W. B. Baker, and A. G. Yodh, "Diffuse Optics for Tissue Monitoring and Tomography," Rep. Prog. Phys. **73**(7), 076701 (2010).
12. T. Durduran and A. G. Yodh, "Diffuse correlation spectroscopy for non-invasive, micro-vascular cerebral blood flow measurement," Neuroimage **85**(Pt 1), 51–63 (2014).
13. F. Jaillon, J. Li, G. Dietsche, T. Elbert, and T. Gisler, "Activity of the human visual cortex measured non-invasively by diffusing-wave spectroscopy," Opt. Express **15**(11), 6643–6650 (2007).
14. T. Durduran, G. Yu, M. G. Burnett, J. A. Detre, J. H. Greenberg, J. Wang, C. Zhou, and A. G. Yodh, "Diffuse optical measurement of blood flow, blood oxygenation, and metabolism in a human brain during sensorimotor cortex activation," Opt. Lett. **29**(15), 1766–1768 (2004).
15. V. Jain, E. M. Buckley, D. J. Licht, J. M. Lynch, P. J. Schwab, M. Y. Naim, N. A. Lavin, S. C. Nicolson, L. M. Montenegro, A. G. Yodh, and F. W. Wehrli, "Cerebral oxygen metabolism in neonates with congenital heart disease quantified by MRI and optics," J. Cereb. Blood Flow Metab. **34**(3), 380–388 (2014).
16. E. M. Buckley, D. Hance, T. Pawlowski, J. Lynch, F. B. Wilson, R. C. Mesquita, T. Durduran, L. K. Diaz, M. E. Putt, D. J. Licht, M. A. Fogel, and A. G. Yodh, "Validation of diffuse correlation spectroscopic measurement of cerebral blood flow using phase-encoded velocity mapping magnetic resonance imaging," J. Biomed. Opt. **17**(3), 037007 (2012).
17. S. A. Carp, G. P. Dai, D. A. Boas, M. A. Franceschini, and Y. R. Kim, "Validation of diffuse correlation spectroscopy measurements of rodent cerebral blood flow with simultaneous arterial spin labeling MRI; towards MRI-optical continuous cerebral metabolic monitoring," Biomed. Opt. Express **1**(2), 553–565 (2010).
18. D. R. Busch, J. M. Lynch, M. E. Winters, A. L. McCarthy, J. J. Newland, T. Ko, M. A. Cornaglia, J. Radcliffe, J. M. McDonough, J. Samuel, E. Matthews, R. Xiao, A. G. Yodh, C. L. Marcus, D. J. Licht, and I. E. Tapia, "Cerebral Blood Flow Response to Hypercapnia in Children with Obstructive Sleep Apnea Syndrome," Sleep **39**(1), 209–216 (2016).
19. R. Choe, M. E. Putt, P. M. Carlile, T. Durduran, J. M. Giammarco, D. R. Busch, K. W. Jung, B. J. Czerniecki, J. Tchou, M. D. Feldman, C. Mies, M. A. Rosen, M. D. Schnall, A. DeMichele, and A. G. Yodh, "Optically measured microvascular blood flow contrast of malignant breast tumors," PLoS One **9**(6), e99683 (2014).
20. R. Delgado-Mederos, P. Zirak, B. Nunez, C. Gregori Pla, J. Marti-Fabregas, L. Dinia, R. Marin Bueno, and T. Durduran, "Real-time transcranial optical monitoring of cerebral blood flow in acute ischemic stroke during and after thrombolysis," Int. J. Stroke **10**, 309–310 (2015).
21. T. Durduran, C. Zhou, B. L. Edlow, G. Yu, R. Choe, M. N. Kim, B. L. Cucchiara, M. E. Putt, Q. Shah, S. E. Kasner, J. H. Greenberg, A. G. Yodh, and J. A. Detre, "Transcranial optical monitoring of cerebrovascular hemodynamics in acute stroke patients," Opt. Express **17**(5), 3884–3902 (2009).
22. T. Durduran, C. Zhou, M. N. Kim, E. M. Buckley, G. Yu, R. Choe, S. M. Durning, S. Mason, L. M. Montenegro, S. C. Nicholson, R. A. Zimmerman, J. Wang, J. A. Detre, A. G. Yodh, and D. J. Licht, "Validation of diffuse correlation spectroscopy for non-invasive, continuous monitoring of cbf in neonates with congenital heart defects," in *Annals of Neurology*(2008), pp. S63–S63.
23. E. M. Buckley, J. M. Lynch, D. A. Goff, P. Schwab, D. R. Busch, S. C. Nicolson, L. M. Montenegro, R. Xiao, A. G. Yodh, J. W. Gaynor, T. L. Spray, and D. J. Licht, "Early postoperative changes in cerebral oxygen metabolism following neonatal cardiac surgery: Effects of surgical duration," J. Thoracic Cardiovascular Surgery **145**, 196–205 (2013).
24. M. Dehaes, H. H. Cheng, E. M. Buckley, P.-Y. Lin, S. Ferradal, K. Williams, R. Vyas, K. Hagan, D. Wigmore, E. McDavitt, J. S. Soul, M. A. Franceschini, J. W. Newburger, and P. Ellen Grant, "Perioperative cerebral hemodynamics and oxygen metabolism in neonates with single-ventricle physiology," Biomed. Opt. Express **6**(12), 4749–4767 (2015).
25. Y. Shang, R. Cheng, L. Dong, S. J. Ryan, S. P. Saha, and G. Yu, "Cerebral monitoring during carotid endarterectomy using near-infrared diffuse optical spectroscopies and electroencephalogram," Phys. Med. Biol. **56**(10), 3015–3032 (2011).
26. N. Roche-Labarbe, S. A. Carp, A. Surova, M. Patel, D. A. Boas, P. E. Grant, and M. A. Franceschini, "Noninvasive optical measures of CBV, StO(2), CBF index, and rCMRO(2) in human premature neonates' brains in the first six weeks of life," Hum. Brain Mapp. **31**(3), 341–352 (2010).
27. E. M. Buckley, N. M. Cook, T. Durduran, M. N. Kim, C. Zhou, R. Choe, G. Yu, S. Schultz, C. M. Sehgal, D. J. Licht, P. H. Arger, M. E. Putt, H. H. Hurt, and A. G. Yodh, "Cerebral hemodynamics in preterm infants during positional intervention measured with diffuse correlation spectroscopy and transcranial Doppler ultrasound," Opt. Express **17**(15), 12571–12581 (2009).
28. T. Durduran, D. L. Minkoff, M. N. Kim, D. Hance, E. M. Buckley, M. Tobita, J. J. Wang, J. H. Greenberg, J. A. Detre, and A. G. Yodh, "Concurrent mri and diffuse correlation & near-infrared spectroscopic measurement of cerebral hemodynamic response to hypercapnia and hyperoxia," in *OSA Biomedical Topicals*(2010).
29. A. Duncan, J. H. Meek, M. Clemence, C. E. Elwell, L. Tyszczuk, M. Cope, and D. T. Delpy, "Optical pathlength measurements on adult head, calf and forearm and the head of the newborn infant using phase resolved optical spectroscopy," Phys. Med. Biol. **40**(2), 295–304 (1995).
30. J. M. Lynch, "Investigations of cerebral hemodynamics in infants with critical congenital heart disease using diffuse optics," in *Physics*(University of Pennsylvania, 2014).
31. C. Zhou, S. A. Eucker, T. Durduran, G. Yu, J. Ralston, S. H. Friess, R. N. Ichord, S. S. Margulies, and A. G. Yodh, "Diffuse optical monitoring of hemodynamic changes in piglet brain with closed head injury," J. Biomed. Opt. **14**(3), 034015 (2009).

Biomedical Optics EXPRESS

32. C. Huang, J. P. Radabaugh, R. K. Aouad, Y. Lin, T. J. Gal, A. B. Patel, J. Valentino, Y. Shang, and G. Yu, "Noncontact diffuse optical assessment of blood flow changes in head and neck free tissue transfer flaps," J. Biomed. Opt. **20**(7), 075008 (2015).
33. P. M. Kirshbom, L. A. Skaryak, L. R. DiBernardo, F. H. Kern, W. J. Greeley, J. W. Gaynor, and R. M. Ungerleider, "Effects of aortopulmonary collaterals on cerebral cooling and cerebral metabolic recovery after circulatory arrest," Circulation **92**(9 Suppl), 490–494 (1995).
34. S. S. Tsui, P. M. Kirshbom, M. J. Davies, M. T. Jacobs, W. J. Greeley, F. H. Kern, J. W. Gaynor, and R. M. Ungerleider, "Nitric oxide production affects cerebral perfusion and metabolism after deep hypothermic circulatory arrest," Ann. Thorac. Surg. **61**(6), 1699–1707 (1996).
35. S. H. Han, B. M. Ham, Y. S. Oh, J. H. Bahk, Y. J. Ro, S. H. Do, and Y. S. Park, "The effect of acute normovolemic haemodilution on cerebral oxygenation," Int. J. Clin. Pract. **58**(10), 903–906 (2004).
36. C. Jenny, M. Biallas, I. Trajkovic, J. C. Fauchère, H. U. Bucher, and M. Wolf, "Reproducibility of cerebral tissue oxygen saturation measurements by near-infrared spectroscopy in newborn infants," J. Biomed. Opt. **16**(9), 097004 (2011).
37. G. Schwarz, G. Litscher, R. Kleinert, and R. Jobstmann, "Cerebral oximetry in dead subjects," J. Neurosurg. Anesthesiol. **8**(3), 189–193 (1996).
38. J. D. Tobias, P. Russo, and J. Russo, "Changes in near infrared spectroscopy during deep hypothermic circulatory arrest," Ann. Card. Anaesth. **12**(1), 17–21 (2009).

1. Introduction

Approximately 10,000 infants per year are born in the United States with a heart defect requiring cardiac surgical intervention in the first year of life [1]. Although advances in surgical techniques have transformed the survival rate so that most of these infants reach school age [2], many of these children exhibit considerable neurodevelopmental deficits later in life [2–4]. Thus, current research focus has shifted to identify opportunities for neuroprotection prior to, during, and following surgery. The choice of surgical technique and rate of cerebral perfusion during cardiopulmonary bypass, for example, have not achieved consensus, and perfusion strategies for complex surgeries generally vary across centers and with surgeon. All perfusion strategies necessitate temporary cessation of cardiac activity (cardioplegia), deep hypothermia (18°C) and a variable duration of temporary cessation of circulation (circulatory arrest). Once all thoracic vessels are identified and isolated, the infant is cannulated for bypass and cardioplegia is instituted. During cardioplegia, cerebral blood flow is entirely dependent on bypass pump flows, but without a direct measure of cerebral blood flow, the clinical team (anesthesiologist, perfusionist and surgeon) cannot optimize pump settings. Cooling is then initiated through the bypass pump followed by a period of circulatory arrest. Some centers perform these delicate surgeries rapidly without resuming circulation (deep hypothermic circulatory arrest, surgical time ~2.2 hr., 1.4 hr. on bypass) while other centers selectively perfuse the brain (selective cerebral perfusion, 6-8 hr. surgery, all on bypass). The literature comparing these techniques and their outcomes is limited, and insights about the process derived from normal physiology are problematic due to congenital defects, the surgery itself, and deep hypothermia. To date, some studies have linked deep hypothermic circulatory arrest (DHCA) exceeding 40 minutes to worse cognitive outcomes and post-operative seizures [5], but these studies have not been replicated for cases wherein deep hypothermia is combined with selective cerebral perfusion techniques.

Critically, physicians have few tools to monitor cerebral hemodynamics during complex surgeries. The neonatal surgical field, in particular, has extreme space constraints, and the head is often covered with ice for cooling and is generally under a surgical drape, limiting access. Commercial cerebral oximeters based on near-infrared spectroscopy (NIRS) are useful as trend monitors and to ascertain optimal cannula positioning [6, 7]. These commercial devices, however, can exhibit considerable inter-device variation [8], and hypothermia may exacerbate inaccuracies due to changes in tissue optical scattering, a parameter which these oximeters generally do not measure. The NIRS instruments also rely on an assumption that hemoglobin species dominate tissue optical absorption [9, 10], but during cessation of circulation, blood is drawn from the venous cannula, sometimes under vacuum, to permit a bloodless surgical field; the minimal intravascular blood, in turn, leads to breakdown of a common assumption that hemoglobin spectra dominates tissue optical absorption. In a different vein, transcranial Doppler ultrasound (TCD) measures blood

Biomedical Optics EXPRESS

velocity in large vessels and is often employed as a surrogate for cerebral blood flow (CBF). Unfortunately, TCD is technically difficult to deploy in the operating room, and TCD signal integrity is especially vulnerable to subtle changes in probe orientation because circumferential probe mounts are not utilized for neonates (due to their soft skulls). Thus, TCD requires nearly constant attention, and energy deposition from continuous TCD throughout the course of surgery is a potential concern. As a result, many centers optimize patient perfusion parameters (*e.g.,* flow rate, blood pressure) without measurement of CBF. Therefore, given the limited range of *in situ* tools and the critical dependence of long term brain injury on cerebral blood flow, there exists a strong clinical need for more quantitative measurement of cerebral hemodynamics throughout the entire course of surgery, including cannulation, cooling, DHCA, rewarming, and resumption of cardiac function.

Diffuse correlation spectroscopy (DCS) is a non-invasive optical technique that employs light intensity fluctuations to measure microvascular blood flow in the cerebral cortex [11, 12]. Previously, DCS has been used to monitor blood flow during cerebral functional activation [13, 14], in hypercapnia [15–18], in cancerous tumors [19], and in adults with ischemic stroke [20, 21]. DCS has also been employed to measure cerebral blood flow in relatively simple clinical scenarios such as neonates prior to and following cardiac surgery [22–24], and during adult carotid endarterectomy [25]. Here we report continuous measurement of microvascular cerebral blood flow in a substantially more complex neonatal surgical arena throughout a planned circulatory arrest and bypass. Critically, the DCS patient interface consists of a simple elastomer pad containing fiber optics that is held on the patient's forehead with clinical tape.

In the present study, our goal is to demonstrate the feasibility of optical diffuse correlation spectroscopy (DCS) for measurement of cerebral blood flow in the highly challenging environment of neonatal open heart surgery. This surgical environment is more complex than the ICU settings and required adaptation of technique and development of patient interfaces. We report a data set collected on a neonate undergoing cardiac surgery with planned selective antegrade cerebral perfusion and circulatory arrest. To our knowledge, this case study is the first demonstration of DCS blood flow monitoring during cardiac or neonatal surgery. The data is comprised of synchronous measurement of DCS microvascular blood flow, TCD macrovascular blood velocity, commercial cerebral oximetry, commercial pulse oximetry, and arterial blood pressure. The DCS data exhibit the full continuum of cerebral blood flow responses, *i.e.,* from near-normal to zero and back to near-normal. Importantly, the work takes first steps towards translation of this optical tool to neuromonitoring in neonatal, pediatric and adult cardiac surgical units and provides a basis for future clinical studies utilizing DCS technology in surgical management. For example, in addition to measurement of the flow biomarker, the DCS optical technique can concurrently interrogate the same cerebral tissues as NIRS and thus, in combination, offers the potential for deriving information about oxygen metabolism during surgery, a factor that could be valuable for understanding and controlling tissue injury.

2. Methods

All data collection was carried out at Texas Children's Hospital under the supervision of the institutional safety review board of the Baylor College of Medicine. The subject was diagnosed with hypoplastic left heart syndrome and informed consent obtained from the subject's parents prior to any research measurements. The subject was male, 3.66 kg, and 10 days old at the time of surgery. Selective antegrade cerebral perfusion was obtained by directing bypass flow through a Gore-Tex graft sewn to the innominate artery and by snaring of the arch vessels at their aortic origin. The subject was placed on bypass for a total of 196 minutes; the cross clamp time was 93 minutes, and the total circulatory arrest time was 15 minutes. The mean bypass flow rate was 580 cc/min (158 cc/kg/min). Total time from beginning of cooling to beginning of rewarming was 145 minutes.

We report data from a two hundred minute period beginning immediately prior to cooling, including circulatory arrest, continuing through resumption of cerebral blood flow with

Biomedical Optics EXPRESS

selective cerebral perfusion at deep hypothermic temperatures, and finally, during rewarming. Systemic vital signs, TCD blood velocity, cerebral oxygen saturation, and DCS cerebral blood flow data were synchronously recorded to a single time-stamped file using the software package ICM + (University of Cambridge, Version 8). Data were analyzed using Matlab (Mathworks Inc., Natick, MA, 2013b).

The primary features of the DCS technique have been described previously [12]. Briefly, the diagnostic utilizes the changing interference of light traveling along different pathways through the medium to calculate blood flow; these effects are manifest in the temporal fluctuations of the multiply scattered light. DCS provides a direct measurement of red blood cells motion; it does not rely on use of models that infer flow from changes in hemoglobin concentration.

The DCS data were fit to a semi-infinite homogeneous medium model for photon propagation in tissue with extrapolated boundary conditions [11]. The tissue absorption and scattering properties utilized in the fits were derived from population averages [26] and were set to 0.1 cm^{-1} and 10 cm^{-1} at 785 nm, respectively. The DCS Blood Flow Index (BFI) is the product of the fraction of scattering events from mobile scatterers (red blood cells) and an effective Brownian diffusion coefficient associated with the mobile scatterers [11]. DCS measurements of blood flow have been validated in neonates against Doppler ultrasound [27] and against both arterial-spin-labeled [28] and phase-encoded velocity mapping MRI [16].

TCD ultrasound data was obtained using a Compumedics DWL Doppler-Box X. Bypass circuit flow was measured with a transonic flowmeter on the arterial limb of the circuit after ultrafiltration. Arterial blood pressure (ABP) was measured with a catheter inserted into the right radial artery (*i.e.,* in the same circulation as the brain). Electrocardiography, central venous pressure and nasal temperature were recorded continuously throughout surgery. Regional cerebral oximetry (rSO_2) was measured using an INVOS (5100C, Covidien) cerebral oximeter. Patient vital signs were recorded with the Carescape B650 (GE). Transcranial Doppler Ultrasound data were captured by analog conversion using data translation DT9800 A/D converter. A schematic of data collection is included in Fig. 1.

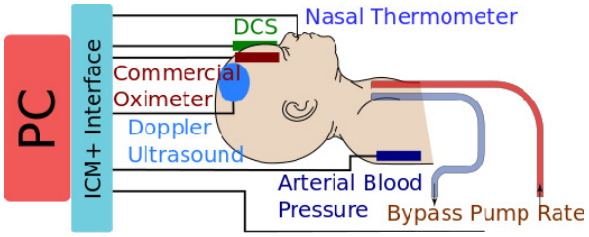

Fig. 1. Schematic of experiment. All data were synchronized temporally using the ICM + interface.

Due to circumstances during surgery, two brief periods of DHCA were captured.

In summary, we report a continuous data set collected from a neonate undergoing cardiac surgery with planned circulatory arrest and selective antegrade cerebral perfusion. These continuous data permit evaluation of the impact of individual interventions on cerebral blood flow. To our knowledge, this case study is the first demonstration of DCS blood flow monitoring during cardiac or neonatal surgery.

Biomedical Optics EXPRESS

3. Results

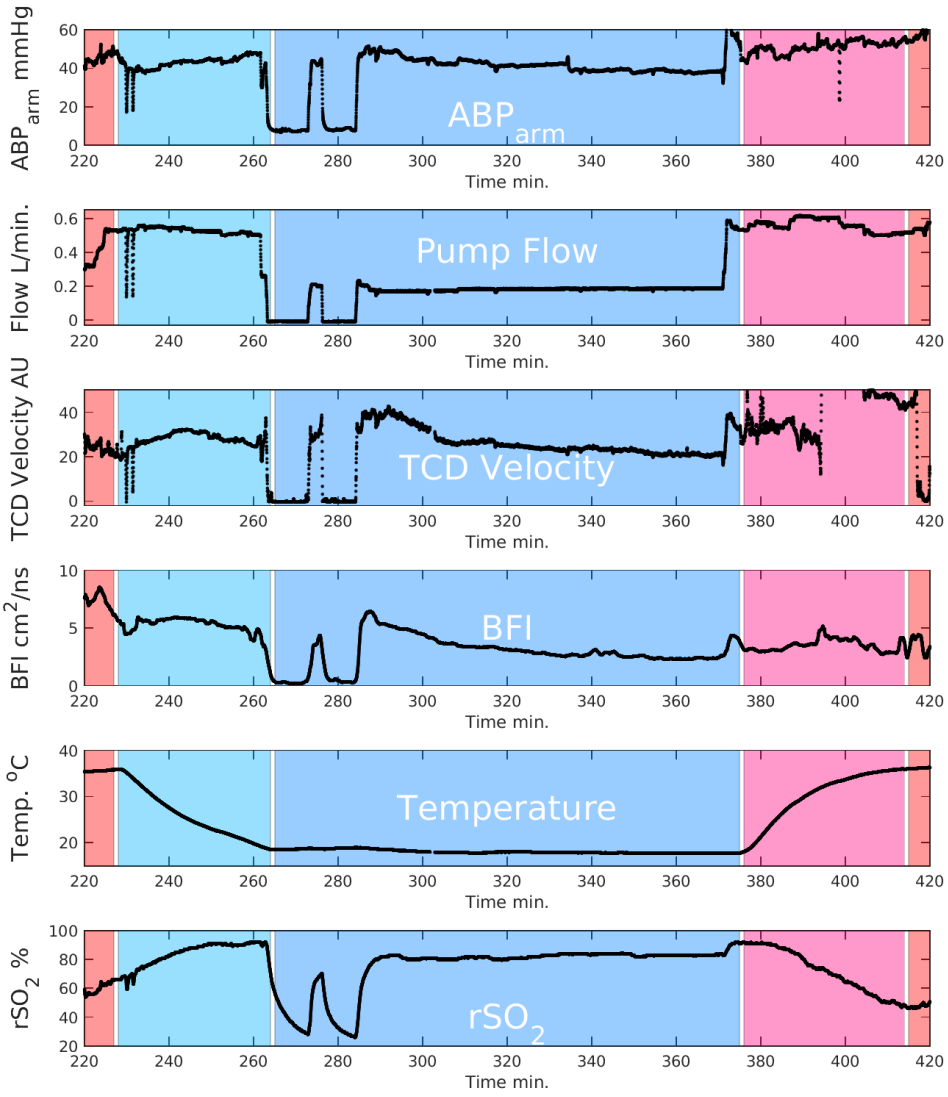

Fig. 2. Time traces of pump flow, arterial blood pressure, TCD ultrasound blood velocity, DCS Blood Flow Index, temperature, and rSO_2 from an INVOS cerebral oximeter. Normothermia, cooling, DHCA, rewarming, and return to normothermia are designated with shaded regions. Data were filtered with a 10-second moving window; motion artifacts were discarded. Note that the rewarming period had significant motion artifacts due to clinical manipulations.

Arterial blood pressures (ABP), bypass pump flow, TCD blood flow velocity, and DCS cerebral blood flow index (BFI) show very similar time courses through the initiation of circulatory arrest and re-initiation of flow (Fig. 2). During circulatory arrest, both DCS blood flow index and TCD blood flow velocity quickly fall to near zero, e.g., the DCS BFI decreased by ~15x during arrest. The rSO_2 exhibited a somewhat slower temporal response to the cessation of flow. We observe (Figs. 2 and 3) that the rSO_2 index increases during cooling to a plateau of ~96%; then during arrest, rSO_2 decreased markedly to ~25%; this decrease is then followed by a return to ~80% during selective perfusion.

Biomedical Optics EXPRESS

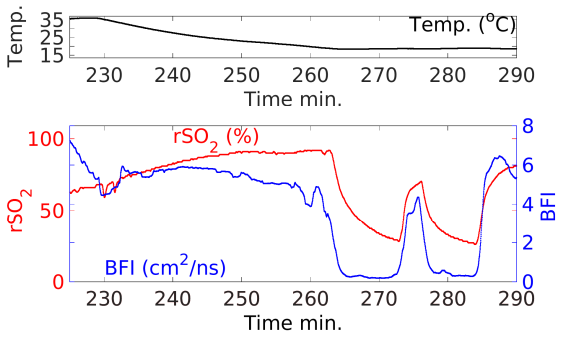

Fig. 3. Expanded view of cooling and arrest periods showing only key parameters. Notice that the measured rSO2 regional oxygenation index rises with falling temperature and returns quickly to near pre-arrest values after initiation of selective perfusion. However, this index does not approach zero during arrest, as might be expected if the drop in RSO2 was due to residual metabolism. At the beginning of circulatory arrest, BFI drops quickly to ~0, while RSO_2 decays more slowly.

Following arrest of the circulation and venous drainage into the reservoir, blood that remains in the head will move to the lowest pressure compartment (posterior large veins). This effect substantially reduces blood volume in the microvasculature that is sampled by the cerebral oximeter (on the forehead). Although the commercial instrumentation utilized in this study is not optimized to measure total hemoglobin content, the changes in the DCS signal time-averaged light *intensity* reflect changes in tissue absorption. During exsanguination, the DCS light intensity increased by ~40%; we can derive a rough estimate for a

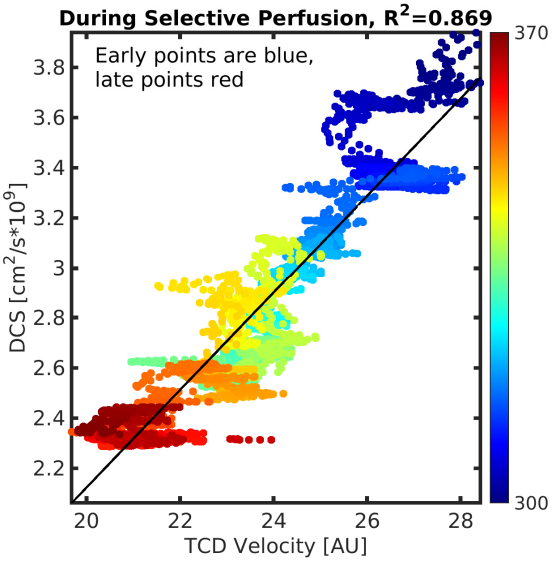

Fig. 4. DCS blood flow vs. TCD during selective perfusion. The color scale indicates time of measurement during the surgical procedure (*i.e.,* ranging from blue (~300 min.) to red (~370 min). The rapid changes in TCD velocity (*i.e.,* the clusters of time points that make horizontal lines in the plot) likely result from subtle orientation shifts of the TCD probe.

hemoglobin concentration change from this data using the Modified Beer-Lambert law (*e.g.,* with a differential pathlength factor of 5 for the neonatal head [29]). With this calculation procedure, we compute a corresponding reduction in the tissue hemoglobin concentration of ~20 μM (*i.e.,* a reduction in blood volume >50%) [30]. It should be noted that these estimates

Biomedical Optics EXPRESS

are not precise and are subject to systematic errors, since patient head properties need not conform to those of subject groups in the source publications.

Finally, we utilized the relatively stable period of selective cerebral perfusion to investigate the relationship between macrovascular blood velocity (TCD) and microvascular blood flow (DCS, Fig. 4). This period was chosen to minimize motion artifacts observed in the TCD signal, e.g., especially those that arise at the cession and resumption of blood flow.

4. Discussion

To our knowledge, this work is the first reported use of DCS to monitor cerebral blood flow during cardiac arrest in a human or in neonatal surgery; related applications of DCS in animal models have been published [31], and a few limited examples of DCS application during simpler human surgeries also exist. Recently for example, Shang [25] observed rapid changes in cerebral blood flow in adults during unilateral carotid endarterectomy (~25%) followed by cerebral blood flow normalization in ~2 minutes. The same group also demonstrated measurement of blood flow in surgical skin flaps [32].

Our DCS measurements of human cerebral blood flow throughout cooling and cessation of circulation represent the largest range of cerebral blood flow yet reported in humans; thus, the work exhibits the dynamic range of the technique during longitudinal monitoring. The large change in the blood flow index (BFI, $50\text{x}10^{-10}\text{cm}^2/\text{s}$ to $3\text{x}10^{-10}\text{cm}^2/\text{s}$, 94%) observed during zero flow periods further validates the use of DCS to assess CBF. Note, the small residual signal during the zero flow period places a bound on the so-called biological-zero that is found to be roughly equivalent to that measured in animal models [31].

We compared TCD and DCS measurements of CBF during the period of selective brain perfusion. The two measurements were strongly correlated ($R^2 = 0.87$, Fig. 4). Since TCD measures large vessels, and since DCS is most sensitive to microvasculature (arterials, capillaries, venules), this agreement suggests that micro- and macro-vascular flows were quite highly correlated in this subject. By contrast, Buckley *et al.*'s study of TCD and DCS measurements of CBF in preterm neonates [27] found a fairly weak correlation ($R^2 = 0.44$). We note that the blood flow perturbation in Buckley's study was gentle (12 deg. tilt of bed), and the infants had comparatively healthy cardiovascular systems. Under such conditions, cerebral blood flow changes may be dampened by autoregulation, resulting in a lower correlation between DCS and TCD. The more dramatic hemodynamic variations and profoundly altered circulation during selective perfusion in the present study, however, likely overwhelms the autoregulatory mechanisms; the correlation between TCD and DCS is consequentially stronger. In the context of clinical translation, we note that DCS provides a reliable non-invasive measurement of the blood flow biomarker, permitting assessment of the efficacy of clinical interventions in real time. Additionally, validation of DCS against TCD across a range of flows from near-normal physiological values through zero has not yet previously been reported in humans. The capability of DCS to measure zero, or near zero, blood flows opens up the possibility to utilize additional biomarkers, including arterial critical closing pressure, throughout the surgical case.

After initiation of selective perfusion (Fig. 2, ~290 min.), both TCD and DCS show a gradual reduction in blood flow over time. Further, the DCS measurements of blood flow stabilize at a level that is ~1/2 of pre-DHCA levels (~50 min. of selective perfusion). This observed post-DHCA reduction in cerebral blood flow is consistent with previous results obtained in animal models [33] in which post-DHCA cerebral blood flow does not recover to the pre-cooling (warm) values. A possible explanation for this observation is an increase in cerebrovascular resistance following DHCA [34]. Of course, the ability to monitor such temporal changes in blood flow during selective perfusion, without the susceptibility to mechanical motion found in TCD data, may lead to improved perfusion strategies.

In Figs. 2 and 3, we observe that during cooling the rSO_2 index increases to a plateau of ~96%, potentially reflecting a decreased metabolism and oxygen consumption at lower temperatures. During arrest, rSO_2 decreased markedly and rapidly to ~25%, followed by a return to ~80% during selective perfusion. The rapid decrease in rSO_2 during circulatory

Biomedical Optics EXPRESS

arrest could suggest that the brain is still metabolically active, *i.e.,* it is still consuming oxygen from non-flowing blood. However, we note that the rSO_2 index does not decrease to zero. Furthermore, rSO_2 rapidly attains near pre-arrest values (~80%) during selective perfusion (290-360 minutes) and remains stable up to the initiation of warming. This discrepancy can be explained by passive drainage of blood from the head and a failure (or partial failure) of the rSO_2 algorithm in the case of near-bloodless tissue. Commercial oximeters, especially trend indicators that clip the rSO_2 at specific values, generally do not provide a mechanism for quantifying tissue absorption and tissue blood volume. One consequence of this limitation is the potential for conflation between drops in rSO_2 due to reduced oxygenation versus reduced blood volume. A large drop in blood volume, for example, can lead to an incorrect reported variation in rSO_2. Therefore, the instrumentation output needs to be interpreted with care during cardiac surgery, as previously noted by Han *et al.,* wherein they found a drop in rSO_2 with reduced hematocrit [35]. The oximeter utilized in the present study is susceptible to this complication, since it measures changes in attenuation at two wavelengths (730 and 810 nm) and at two source-detector separation distances. By contrast, typical research-grade systems utilize additional wavelengths and derive information about photon path length for improved quantification of hemoglobin concentration and oxygen saturation and thus an improved assignment of tissue oxygenation.

Other work in the literature [8, 36, 37] also suggests that rSO_2 measurements from continuous wave oximeters are not reliable indicators of absolute tissue oxygenation. Preliminary results from the present study suggest that this effect is worsened when cerebral blood volume is low. Again, this observation is consistent with previous work that identified a drop in rSO_2 during reduction of hematocrit [35]. Therefore, during major cardiac surgery wherein episodes of low cerebral blood volume are expected, the use of rSO_2 as a measure of oxygen delivery must be interpreted with care. Earlier findings [38], for example, that noted increased mortality and morbidity following sustained periods with $rSO_2 < 45\%$, might actually indicate risk from low blood volume rather than low blood oxygen saturation. This limitation associated with the saturation index suggests that a transition to more sophisticated monitoring tools, such as time- or frequency-domain diffuse optical spectroscopy which quantify both blood volume and saturation and tissue scattering in each individual [11], is desirable. Additionally, combining these more quantitative NIRS measurements with reliable DCS measurements of blood flow will enable calculation of tissue oxygen metabolism.

These data have limitations. Perhaps most significantly, the data lack a concurrent continuous measurement of tissue absorption and scattering during throughout the measurement period. The continuous-wave two wavelength cerebral oximeter utilized in this study does not measure hemoglobin concentration or tissue scattering; as discussed above, this limitation could potentially cause a conflation between tissue blood oxygenation and blood concentration in the rSO_2 index. At best, such cerebral oximeters are trend monitors and ought to be used as such [36]. Errors in estimation of tissue optical properties can shift the calculated value of BFI, although such errors have much less impact on the fractional changes of blood flow discussed here (accounting for the change in blood volume increases the change in BFI by ~2%). Future work will incorporate a time- or frequency-domain diffuse optical spectroscopy system in conjunction with the DCS system to permit simultaneous quantification of hemoglobin concentration and saturation, tissue optical properties, and blood flow. Additionally, it is desirable for future studies to include collection of EEG with optical data.

In summary, we have demonstrated the feasibility of continuous, real-time, intra-operative optical measurements of cerebral blood flow during neonatal cardiac surgery. The results meet expectations for the surgical perturbations employed, demonstrate the first measurement of cerebral blood flow in humans from near zero to near normal flow, and the work takes valuable steps towards development of optical instrumentation to non-invasively probe cerebral hemodynamics in real-time during cardiac and neonatal surgery. The instrumentation, both alone or in combination with NIRS, provides access to flow and metabolic biomarkers and thus holds potential to provide clinicians with information needed

Biomedical Optics EXPRESS

to adjust neuroprotective therapy in situ for individual patients. Such individualized continuous therapeutic guidance, for example, could enable clinicians to titrate therapy for optimization of cerebral health.

Funding

National Institutes of Health (NIH, R01-NS072338, HL007915, R01-NS060653 & P41-EB015893), the Thrasher Foundation, Institute of International Education, and philanthropic support from the June and Steve Wolfson Family Foundation.

Acknowledgments

The authors thank the study participant and family. We also thank Dr. Jennifer Lynch, Dr. Ashwin Parthasarathy, Tiffany Ko, Dr. Constantine Mavroudis, Dr. Turgut Durduran, and Dr. Genevieve Du Pont-Thibdeau.